University of Groningen

Local Group galaxies in a LambdaCDM Universe

Li, Yang-Shyang

IMPORTANT NOTE: You are advised to consult the publisher's version (publisher's PDF) if you wish to cite from it. Please check the document version below.

Document Version
Publisher's PDF, also known as Version of record

Publication date:
2009

Link to publication in University of Groningen/UMCG research database

Citation for published version (APA):
Li, Y-S. (2009). *Local Group galaxies in a LambdaCDM Universe*. s.n.

Copyright
Other than for strictly personal use, it is not permitted to download or to forward/distribute the text or part of it without the consent of the author(s) and/or copyright holder(s), unless the work is under an open content license (like Creative Commons).

The publication may also be distributed here under the terms of Article 25fa of the Dutch Copyright Act, indicated by the "Taverne" license. More information can be found on the University of Groningen website: https://www.rug.nl/library/open-access/self-archiving-pure/taverne-amendment.

Take-down policy
If you believe that this document breaches copyright please contact us providing details, and we will remove access to the work immediately and investigate your claim.

Downloaded from the University of Groningen/UMCG research database (Pure): http://www.rug.nl/research/portal. For technical reasons the number of authors shown on this cover page is limited to 10 maximum.

Download date: 05-05-2023

4

On the common mass scale of the Milky Way satellites

Abstract*

We use a hybrid approach that combines high-resolution simulations of the formation of a Milky Way-like halo with a semi-analytic model of galaxy formation to study the mass content of dwarf galaxies in the concordance ΛCDM cosmology. We find that the mass within 600 pc of dark matter haloes hosting luminous satellites has a median value of $\sim 3.2 \times 10^7\,\mathrm{M}_\odot$ with very little object-to-object scatter. In contrast, the present day total luminosities of the model satellites span nearly five orders of magnitude. These findings are in very good agreement with the results recently reported in the literature for the dwarf spheroidal galaxies of the Milky Way. Dwarf irregular galaxies like the Small Magellanic cloud are predicted in our model to have a similar, if only slightly larger dark matter mass within 600 pc.

Key words: cosmology:theory – dark matter – galaxies:general – galaxies:dwarf

* Based on Li, Helmi, De Lucia & Stoehr 2008, submitted to MNRAS *Letters* on 7th October, 2008

4.1 Introduction

THE dwarf satellite galaxies of the Milky Way are the most dark matter dominated systems known to date in the Universe. They represent a heterogeneous population in terms of their stellar properties such as luminosity, star formation and chemical enrichment histories (Mateo, 1998; Dolphin et al., 2005; Martin et al., 2008). Yet, the mass enclosed within a radius of 300 (or 600) pc appears to be roughly constant (Gilmore et al., 2007; Strigari et al., 2007, 2008). This could imply a minimum mass scale for the existence of dwarf spheroidal galaxies, as originally suggested by Mateo (1998). It is currently unclear whether this is due to the microphysics of the dark matter particles, or to astrophysical processes that inhibit star formation on small scales.

For Weakly Interacting Massive Particles (WIMPs), free streaming is expected to cut off the power spectrum at masses of $\sim 10^{-6}\,\mathrm{M}_{\odot}$ (e.g. Green et al., 2005) or smaller. Then, in models which assume these as dark matter particles (e.g. WDM, ΛCDM), a minimum mass scale for dwarf spheroidals can only result as a consequence of astrophysical processes that affect the collapse of baryons and the formation of stars on small galactic scales. For example, the presence of a strong photo-ionizing background (possibly associated to the reionization of the Universe) can suppress accretion and cooling in low-mass haloes. This is because the heating of the gas will raise its pressure and therefore may suppress its collapse in haloes with virial velocities $\lesssim 30 - 50\ \mathrm{km\,s^{-1}}$ (e.g. Efstathiou, 1992; Quinn et al., 1996; Thoul & Weinberg, 1996; Gnedin, 2000; Okamoto et al., 2008, and references therein). This has often been considered as a possible solution to the excess of small scale structures found in CDM and in particular in N-body simulations of galaxy size systems (Kauffmann et al., 1993; Klypin et al., 1999; Moore et al., 1999; Bullock et al., 2000; Somerville, 2002; Benson et al., 2002). In addition, in systems with virial temperature below 10^4 K gas cannot cool via hydrogen line emission, and must rely on the highly inefficient cooling through collisional excitations of H_2 molecules (Haiman et al., 2000; Kravtsov et al., 2004).

In this Chapter we discuss the existence of a common mass scale for Milky Way satellites using results from high resolution N-body simulations of galaxy-size haloes coupled with semi-analytic techniques to model the evolution of the baryonic component of galaxies. This approach allows us to identify the dark matter substructures that host stars and to characterise their stellar properties. At the same time, the high resolution of the simulations used in this study permits a reliable determination of the internal dynamical properties of these satellites. As we shall describe below, we find that the dark matter mass within 600 pc for the model satellites shows very little scatter from object to object. This is in very good agreement with the observational results by Strigari et al. (2007, 2008). Interestingly, our model also reproduces the very wide range of luminosities observed for the satellite galaxies around the Milky Way.

4.2 The Simulation and the Galaxy Formation Model

In this study, we use a high-resolution resimulation of a 'Milky Way' halo from the GA series described in Stoehr et al. (2002) and Stoehr et al. (2003). The candidate 'Milky Way' halo was selected as a relatively isolated halo with a 'quiet' merging history (last major merger at $z > 2$) and with maximum rotational velocity close to $\sim 220\,\mathrm{km\,s^{-1}}$. The halo, selected from an intermediate resolution cosmological simulation, was then re-simulated at four progressively higher resolutions using the 'zoom' technique (Tormen, Bouchet & White, 1997). The underlying cosmological model is a flat Λ-dominated CDM Universe with cosmological parameters: $\Omega_{\mathrm{m}} = 0.3$, $\Omega_{\Lambda} = 0.7$, $H_0 = 70\,\mathrm{km\,s^{-1}\,Mpc^{-1}}$, $n = 1$, and $\sigma_8 = 0.9$. In this study, we use the highest resolution simulation of the series - GA3new - which contains $\sim 10^7$ particles within the virial radius.

As explained in De Lucia & Helmi (2008), the simulated halo is more massive ($M_{200} \sim 3 \times 10^{12}\,\mathrm{M_{\odot}}$) than recently estimated for our Galaxy (Battaglia et al., 2005; Xue et al., 2008). Following Helmi et al. (2003), we then scale our 'Milky Way' halo by adopting a scaling factor in mass $M_{200}/M_{\mathrm{MW}} = \gamma^3 = 2.86$. This implies that we scale down the positions and velocities by a factor $\gamma = 1.42$. The Plummer equivalent softening length for the scaled simulation is 0.18 kpc. The scaled particle mass is $1.03 \times 10^5\,\mathrm{M_{\odot}}$.

Simulation data (stored in 108 outputs between $z = 37.6$ and $z = 0$) were analysed using a standard friends-of-friends algorithm and the substructure finder algorithm SUBFIND (Springel et al., 2001a). As in previous work, we have considered all substructures retaining at least 20 self-bound particles - which sets the substructure mass limit to $2.06 \times 10^6\,\mathrm{M_{\odot}}$, for the scaled simulation. Finally, these halo catalogues have been used to construct the halo merger trees that represent the basic input for the galaxy formation model used in this study. For details on the post-processing, we refer the interested reader to Springel et al. (2005) and to De Lucia & Blaizot (2007).

The galaxy formation model used in our study is a refinement of the model described in De Lucia & Helmi (2008), who have studied the predicted physical properties of the Milky Way and of its stellar halo using the same set of re-simulations used here. This model builds upon the methodology introduced in Springel et al. (2001a) and De Lucia et al. (2004a) and has been further refined in later years. The interested reader is referred to Croton et al. (2006), De Lucia & Blaizot (2007), and De Lucia & Helmi (2008) for a detailed account of the modelling of the various physical processes considered. In order to obtain a better agreement with the observed properties of the Milky Way satellites, a few refinements were made to the model used in De Lucia & Helmi (2008). For completeness, we give here a short description of these refinements that are described in detail in Chapter 3.

- As described in Croton et al. (2006), reionization was modelled using the formulation provided by Kravtsov et al. (2004) and was previously assumed to start at redshift 8 and to be completed by redshift 7. In the study presented here, we assume an 'early' reionization which starts at redshift 15, and is

complete by redshift 11.5 (Spergel et al., 2007).

- In previous studies, haloes with virial temperature below 10^4 K were allowed to cool at the rates corresponding to 10^4 K. In this study, we completely suppress cooling in these low-mass haloes (e.g. Haiman et al., 2000).

- In previous implementations of our galaxy formation model, all metals produced by new stars were instantaneously mixed to the cold gas (De Lucia et al., 2004a; De Lucia & Helmi, 2008). Inspired by the numerical simulations of Mac Low & Ferrara (1999), in this study we assume that for galaxies embedded in haloes with virial mass below $5 \times 10^{10}\,\mathrm{M}_\odot$, most of the new metals (95%) are ejected into the hot gas phase.

As we haven shown in Chapter 3, these refinements result in a satellite population with physical properties that closely resemble those observed for the Milky Way satellites, while leaving essentially unaltered the characteristics of the model Milky Way discussed in De Lucia & Helmi (2008).

4.3 Results

Fig. 4.1 shows the mass function of all substructures identified at redshift zero within 280 kpc from the central galaxy and lying in the same FOF group (dashed histogram), and the corresponding mass function of satellites (i.e. subhaloes hosting stars) in our model (solid histogram). The subhalo masses plotted in Fig. 4.1 are computed summing up the masses of all self-bound particles, and scaled as discussed in Sec. 4.2. Fig. 4.1 shows that the dark matter masses of our satellites span a relatively large range from $\sim 5 \times 10^6\,\mathrm{M}_\odot$ to $\sim 5 \times 10^{10}\,\mathrm{M}_\odot$, and that the distribution is nearly flat between 10^7 and $10^9\,\mathrm{M}_\odot$. In contrast, the subhalo mass function continues to rise steeply up to the resolution limit of our simulation. The simulation used in this study contains almost 2000 subhaloes in the considered region, but our model predicts that only 51 of them host stars. This is still larger (by a factor of about 2) than the number of Milky Way satellites currently known. However, when corrections due to incompleteness are considered, this discrepancy in number is eliminated (Koposov et al., 2008).

The high resolution of the simulation used in this study allows us to measure the satellite's dark matter mass enclosed within a (small) given radius. Following Strigari et al. (2007), we measure the mass within 600 pc, which corresponds to 3.33 (scaled) softening lengths. We do not attempt to measure the mass within 300 pc, as done in the more recent analysis by Strigari et al. (2008), as this would be beyond reach for the GA3new simulation.

In order to measure the mass within 600 pc ($M_{0.6}$ hereafter), we compute the centre of mass position for each subhalo using its 10 per cent most bound particles. We then count the number of bound particles located within 600 pc from the centre of mass of each subhalo, and multiply this number by the particle mass. We find

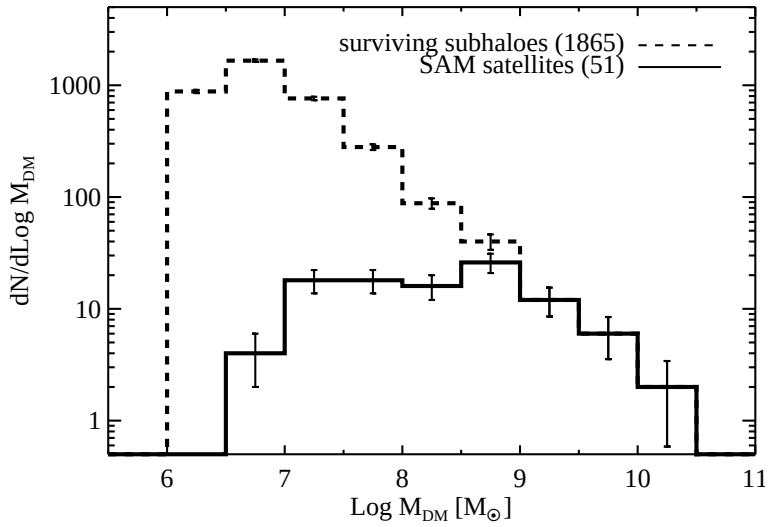

Figure 4.1: The solid histogram shows the present-day mass function for the satellites in our model. Error bars show the corresponding 1 - σ Poisson uncertainties. The dashed histogram shows the subhalo mass function, which steeply rises up to the resolution limit of our simulation.

that our subhaloes have on average ~ 380 particles within this distance, and in nine cases $\lesssim 100$ particles.

Numerical effects will in general tend to artificially lower the mass in the inner regions of subhaloes. We believe, however, that our measurements are robust and are not strongly affected by the limited numerical resolution. In order to quantify the effect of numerical resolution on our estimates of $M_{0.6}$, we assume that the inner density profiles of subhaloes are well fit by Einasto profiles, as recently demonstrated by Springel et al. (2008) using the very high-resolution simulations of the Aquarius project. The Einasto profile can be fully characterised with 3 parameters, namely the logarithmic slope α, the peak circular velocity $V_{\rm max}$ and the radius $r_{\rm max}$ where this peak value is reached. Springel et al. (2008) find $\alpha \sim 0.15 - 0.25$, with an average value of ~ 0.18. Assuming this value for α, and measuring $V_{\rm max}$ and $r_{\rm max}$ directly from the simulation used in this study, we obtain an independent estimate of $M_{0.6}$.

When we compare the $M_{0.6}$ values derived using the Einasto profile with those directly measured in the simulation, we find at most a factor two increase, but in most cases the difference is less than 40%. The largest deviation is found for a subhalo nearing disruption and whose circular velocity curve is particularly noisy. For this object, as well as for those subhaloes with rotation curves within 600 pc (and $M_{0.6}$) that have evolved significantly in the last 2 Gyrs (these are in general the least massive objects), we always indicate both the direct measurement of $M_{0.6}$ as well as the value derived using the Einasto profile. For the rest of the systems,

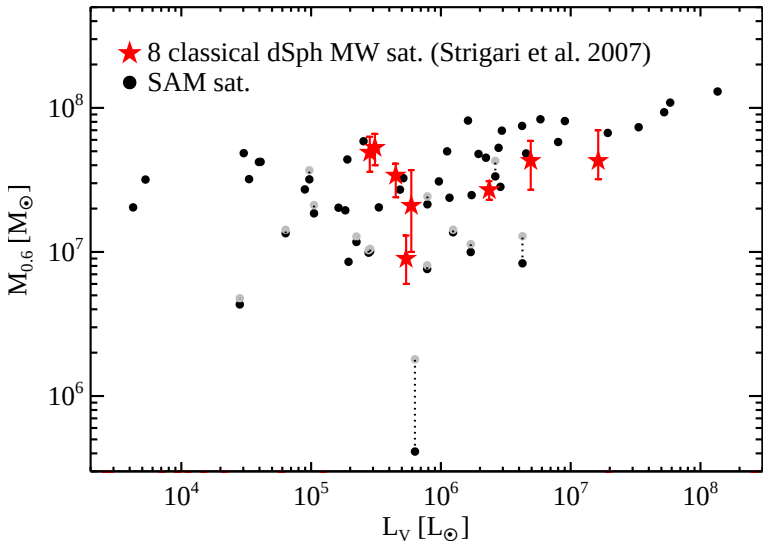

Figure 4.2: Mass within 600 pc as a function of the V-band luminosity for our model satellites (black and grey solid circles), and for the eight brightest dwarf spheroidal galaxies of the Milky Way (asterisks), where the Sagittarius dwarf has been excluded because it is clearly not in dynamical equilibrium. Black solid circles correspond to $M_{0.6}$ measured via direct particle counting. For the model satellites which show clear signs of tidal disruption of the associated subhaloes, we also plot the Einasto $M_{0.6}$ estimates shown with grey symbols.

we keep the direct measurements only. It is important to note that the corrections derived from the Einasto model are nevertheless smaller than the scatter found in the values of $M_{0.6}$ within the population of model satellites.

Fig. 4.2 shows the measured $M_{0.6}$ for satellites as a function of the total V-band luminosity predicted by our galaxy formation model. Black symbols show the values of $M_{0.6}$ measured directly from the simulations. As discussed above, for satellites with signs of tidal disruption we also show the corresponding values estimated assuming an Einasto profile with $\alpha = 0.18$. These are the grey symbols linked to the direct measurement by dotted lines. In this Figure we have excluded two objects whose stellar masses, as derived from the galaxy formation model, are larger than the dark matter mass of the associated subhalo. These objects are nearly fully disrupted in the numerical simulation, but since we do not follow the tidal stripping of the stars in our model, we overestimate their current luminosity by an unknown factor.

Our model satellites span more than four orders of magnitude in luminosity, which is comparable to that observed for the dwarf galaxies around the Milky Way when one includes the recently discovered 'ultra-faint satellites'. In contrast, their dark matter masses within 600 pc do not differ by more than one decade. The asterisks in Fig. 4.2 show the estimates given by Strigari et al. (2007) for the clas-

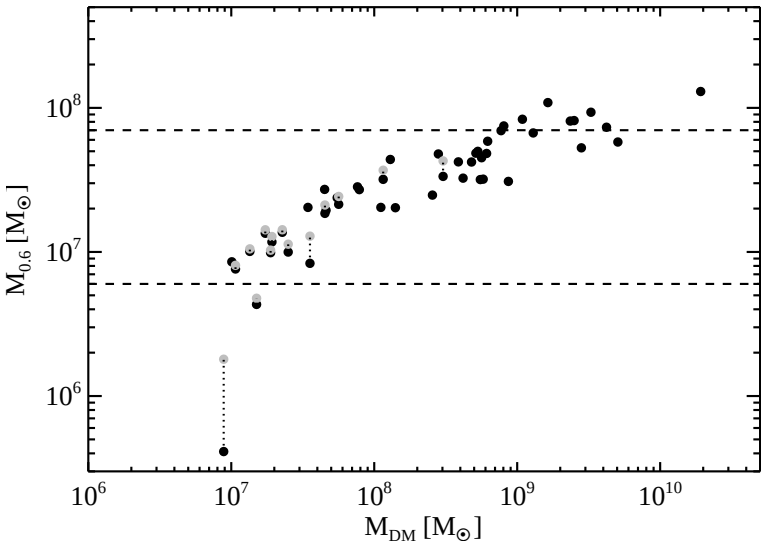

Figure 4.3: Mass within 600 pc as a function of the total mass estimated by SUBFIND. The two dashed lines correspond to the upper and lower limits for the observational estimates of $M_{0.6}$ for the 8 classical MW dSphs (Strigari et al., 2007). Symbols are the same as in Fig. 4.2.

sical dwarf spheroidal satellites of the Milky Way. Our results are therefore entirely consistent with previous analyses claiming the existence of a minimum mass scale of the order of $10^7\,\mathrm{M}_\odot$, and no (or very few) subhaloes (in equilibrium) hosting stars below this threshold (Mateo, 1998; Strigari et al., 2007; Gilmore et al., 2007; Strigari et al., 2008). We note that the correlation between $M_{0.6}$ and the V-band luminosity in the model is somewhat stronger than in the real data. In the context of our model, satellites with smaller $M_{0.6}$ values could exist, but these would generally expected to be strongly tidally perturbed, i.e. out of dynamical equilibrium. Note that in Fig. 4.2 we have also included model satellites that could be the counterparts of systems like the Small Magellanic Cloud (i.e. gas-rich). In our model, such luminous objects are expected to be embedded in the most massive subhaloes at the present time. Hence Fig. 4.2 shows that we predict that the Small Magellanic Cloud should have only slightly larger values of $M_{0.6}$, namely $\sim 10^8\,\mathrm{M}_\odot$, in comparison to the dwarf spheroidals surrounding the Milky Way.

An intriguing question is whether this result implies that the Milky Way satellites reside in dark matter haloes of the same total mass. We address this question in Fig. 4.3 where we show the estimated $M_{0.6}$ as a function of the total dark matter mass given by SUBFIND for the objects shown in Fig. 4.2. While for most model satellites $M_{0.6}$ varies in the range $\sim 10^7 - 10^8\,\mathrm{M}_\odot$, their total mass spans three orders of magnitude (from $\sim 10^7$ to $\sim 10^{10}\,\mathrm{M}_\odot$). Therefore, in our model, a common mass within 600 pc does not imply the same total mass. This is because this scale is generally too small compared to the full extent of dark matter subhaloes hosting

luminous satellites. In other words, satellites are not embedded in dark matter subhaloes that can be characterised by a single parameter, since the relationship between concentration and virial mass is not very tight for these objects.

Our model satellites are found to be embedded in dark matter haloes whose present total mass is larger than $\sim 10^7\,\mathrm{M}_\odot$. Strigari et al. (2008) have suggested that this could imply that these objects had a characteristic mass of $\sim 10^9\,\mathrm{M}_\odot$ at the time of accretion (i.e. when they became satellites of the Milky Way). In our model, we find a broad range of total dark matter mass at the time of accretion for our luminous satellites, that extends from $\sim 3\times10^8\,\mathrm{M}_\odot$ up to $6\times10^{10}\,\mathrm{M}_\odot$. The existence of a minimum mass scale for model satellites is essentially the result of a combination of the two aforementioned physical processes: cooling is strongly inhibited for haloes with $T_{\rm vir} < 10^4$ K, and reionization prevents the further collapse of gas onto low-mass haloes.

The wide range of total dark matter masses observed today reflects in part the initial broad range of masses of the satellites' haloes. Furthermore, the tidal field of the Galaxy halo will act to increase the difference in present-day mass of these objects depending on when they were accreted as well as on their orbits (De Lucia et al., 2004a; Gao et al., 2004b). For example, our faintest objects, which are typically also the least massive today, were accreted earlier and have suffered significant stripping. On the other hand the brightest satellites reside in the most massive haloes, have typically been accreted only recently and therefore have not been significantly affected by tides.

4.4 Conclusions

We have used a high-resolution simulation of the formation of a Milky Way-like halo in combination with a semi-analytic model of galaxy formation in order to study the mass content of subhaloes hosting luminous satellites. The galaxy formation model used in this study shows considerable agreement with a large number of observed galaxy properties (see discussion in De Lucia & Helmi 2008 and references therein). With the few refinements discussed in Section 4.2, the same model is able to reproduce quite well the physical properties of the observed Milky Way satellites (Chapter 3) while leaving essentially unaltered the level of agreement with observational data shown in previous work.

The key result of this Chapter is that our model predicts naturally a common dark matter mass scale within 600 pc for the luminous satellites. Our model satellites span nearly five orders of magnitude in luminosity, while their dark matter masses within 600 pc vary only by one decade (between $\sim 10^7$ and $\sim 10^8\,\mathrm{M}_\odot$), in very good agreement with recent observational measurements. The total dark matter masses of our luminous satellites, however, span about three orders of magnitude with the scatter reflecting the lack of a tight concentration-virial mass relation, the different accretion times, and the different amounts of tidal stripping suffered by the parent substructures once they have fallen onto the Milky Way halo. The existence of such a scale in the context of our model results from the strong sup-

pression of accretion and cooling of gas by low-mass haloes after reionization, as well as from the atomic hydrogen cooling threshold at $T_{\rm vir} = 10^4$ K. These physical processes then inhibit the formation of stars in objects that never reached virial velocities above $\sim 17\,{\rm km\,s^{-1}}$.

We note that our analysis has been carried out considering the mass within 600 pc, and an even tighter distribution may be expected when measuring the mass within 300 pc as used in the most recent study by Strigari et al. (2008). This mass scale is beyond the resolution limit of the simulation used in this Chapter but is within reach of the new generation of ultra-high resolution simulations like those carried out within the Aquarius project.

Acknowledgments

Giuseppina Battaglia, Volker Springel and Simon White are gratefully acknowledged for interesting discussions and useful comments. This work has been partially supported by the Netherlands Organisation for Scientific Research (NWO). AH wishes to thank the hospitality of the KITP, where this work reached its final form.